

## “Aligned-to-random” nanofiber scaffolds for mimicking the structure of the tendon-to-bone insertion site

**Jingwei Xie<sup>1</sup>, Xiaoran Li<sup>1</sup>, Justin Lipner<sup>2</sup>, Cionne N. Manning<sup>2</sup>, Annie G. Schwartz<sup>1</sup>, Stavros Thomopoulos<sup>\*2</sup> and Younan Xia<sup>\*1</sup>**

<sup>1</sup> Department of Biomedical Engineering, Washington University, St. Louis, Missouri 63130, USA

<sup>2</sup> Department of Orthopaedic Surgery, Washington University, St. Louis, Missouri 63110, USA

\*E-mails: xia@biomed.wustl.edu, ThomopoulosS@wudosis.wustl.edu

### Materials and Methods

#### Fabrication and characterization of nanofibers

The nanofibers were produced by electrospinning and the setup was similar to what we used in previous studies.<sup>1-3</sup> PLGA with L:G molar ratios of 50:50, 65:35, 75:25, and 85:15 (Sigma-Aldrich, St. Louis, MO) was dissolved in a solvent mixture consisting of dichloromethane (DCM) and N, N-dimethylformamide (DMF) (Fisher Chemical, Waltham, MA) with a ratio of 8:2 (v/v) (at a concentration 25% (w/v)). The polymer solution was pumped at a flow rate of 0.5 mL/h using a syringe pump. A DC high voltage of 12 kV was applied between the nozzle (a 22-gauge needle) and a grounded collector. Different collectors were employed to generate different types of nanofiber assemblies. Random nanofibers were directly collected using cover glass slips. A stainless steel frame (with an open void of 2 cm × 5 cm) was used as the collector. Subsequently, the aligned nanofibers were transferred to cover glass slips by lifting up the fibers from underneath. Random and aligned scaffold samples for mechanical tests were collected with a rotating mandrel at a rotating speed of 200 rpm for the random sample or 2000 rpm for the aligned sample. Samples containing both aligned and random fibers next to each other (“aligned-to-random scaffolds”) were obtained by using two stapler-shaped metals separated by an air gap. Fibers were deposited in random and aligned orientations on the metal and across the air gap,

The morphologies and structures of various fiber assemblies were characterized by scanning electron microscopy (SEM) (200 NanoLab, FEI, Oregon). To avoid charging, the polymer fiber samples were coated with platinum using a sputter coater for 40 seconds in vacuum at a current intensity of 40 mA after the sample had been fixed on a metallic stud with double-sided conductive tape. The accelerating voltage was 15 kV for the imaging process.

### **Mechanical property characterization**

Electrospun PLGA samples were cut into 3 mm wide strips with a scalpel blade using a positive template. The sample thickness was measured using a laser micrometer (LK-081, Keyence, NJ) to a resolution of  $\pm 3$   $\mu\text{m}$ . In order to grip the samples, the ends were covered with 220 grit sandpaper. To track deformation, a texture-rich pattern of alizarin (15 g/L) was sprayed onto the test strips using a metered misting spray. Mechanical testing was performed in uniaxial displacement-control tension using a custom-built apparatus. Video was captured at 2.5 Hz with a resolution of 1360 x 1024 pixels. Time, displacement, and force data was captured at 10 Hz and synchronized with the video. The gage length of the samples was  $13.7 \pm 1.8$  mm, yielding an aspect ratio of  $4.6 \pm 0.6$ . The samples were pulled in tension at a displacement rate of 0.1 mm per sec until failure (i.e., at a strain rate of  $\sim 0.7$  %/sec). The force, displacement, and image data were analyzed using custom code written in Matlab (The Mathworks, Natick, MA). Engineering stress was calculated as force divided by cross-sectional area. Zero-strain displacement was defined as the displacement at 3% of ultimate force. Video frames were exported into a texture correlation program that located points in both the reference ( $\varepsilon = 0\%$ ) and the deformed frames with a resolution of 0.25 pixels. Deformed images were sampled from the linear region of the stress-strain curve, with intervals of 0.4 sec. Displacement data was exported into a custom Matlab program which used the nine nearest points to find the Lagrangian finite strain of that region:  $E_{ij} = 0.5 (F_{ki} F_{kj} - \delta_{ij})$ . The strain was plotted against the corresponding stress and the slope of the best-fit line was determined to define the local modulus in the direction of tension at that point. To avoid artifacts due to gripping, the average modulus for the central 70% of each scaffold was determined. On average,  $189 \pm 131$  points were used per sample to calculate modulus. There was a strong linear correlation when comparing local modulus with “grip-to-grip” modulus (i.e., where strain was calculated simply from the grip-to-grip displacement data)

( $R^2=0.9$ ). However, due to artifacts from the grip (as is typical in soft tissue mechanics), the grip-to-grip modulus underestimated the true modulus by ~40%.

### **Tendon fibroblast culture**

Rat supraspinatus and infraspinatus tendon samples were cut into ~1 mm<sup>3</sup> cubes and trypsinized for 5 min; the trypsin activity was then neutralized by 10% fetal bovine serum (FBS) in DMEM. The tissue explants were placed in a 35 mm culture dish, and covered with a medium, containing 10% FBS at 37 °C, 95% O<sub>2</sub>, 5% CO<sub>2</sub>. After the fibroblasts migrated out from explant tissues and grew to a confluent monolayer, they were released by 0.25% trypsin/EDTA and centrifuged at 1000 rpm for 5 min. The tendon fibroblasts were then resuspended in a medium with 10% FBS and then seeded onto a 75 cm<sup>2</sup> culture flask for subculture.

### **Cell proliferation**

Tendon fibroblast cells in culture flask were grown to 80% confluence and then  $4 \times 10^4$  cells were transferred to wells of a 24-well plate containing one circular fiber scaffold each with a diameter of 15 mm (N = 4 per group). Medium was changed every other day. The plate was incubated for 1, 3, and 7 days. At different time points, the medium was removed from the well and thirty microliters of MTT assay and 270 ml of medium were then added to each well. After incubation for 3-4 h, the solution was removed, thus leaving the precipitate behind. One hundred microliters isopropanol was then added to each well before the plate was observed using a microplate reader. Cell viability was determined by the value of absorbance at 560 nm, which represented the amount of formazan generated by the cells proliferated on the fiber scaffold.

### **Cell morphology**

At day 3 and day 7, the cells were stained with Fluorescein Diacetate (FDA). Alternatively, the cells were fixed by 3.7% formaldehyde and then stained F-actin with Alexa Fluor® 488 phalloidin in green and cell nucleus with 4'-6-Diamidino-2-phenylindole (DAPI) in blue, respectively (N = 4 per group). Fluorescence images were taken using a QICAM Fast Cooled Mono 12-bit camera (Q Imaging, Burnaby, BC, Canada) attached to an Olympus microscope with OCapture 2.90.1 (Olympus, Tokyo, Japan). To examine cell morphology, the cell shape factor (CSF) was calculated as follows:  $CSF = 4 \times \pi \times S / P^2$ , where S is the area of the cell and

P is the perimeter of the cell.<sup>4</sup> The area and perimeter of cell was obtained using Image J software (National Institutes of Health, MD). Orientation of cellular alignment was calculated using a custom written Matlab program based on previous studies.<sup>5</sup>

### **Immunohistochemistry**

Production of collagen type I or II by the tendon fibroblasts on the fiber scaffolds was assessed using immunohistochemistry. At day 7, the cells were rinsed with PBS and fixed with 3.7% formalin for 1 h (N = 4). Cells were permeabilized using 0.1% Triton X-100 (Invitrogen) in PBS for 20 min, followed by blocking with PBS containing 5% normal goat serum (NGS) for 30 min. Monoclonal antibodies for type I collagen (1:20 dilution) and type II collagen (1:100) were obtained from EMD Chemicals (Calbiochem, San Diego, CA) and Sigma-Aldrich, respectively. Cells were washed three times with PBS containing 2% FBS. The secondary antibodies Gt × Rb IgG Fluor and Gt × Rat IgG Cy3 (H+L) (Chemicon, Temecula, CA) (1:200 dilution) were applied for 1 h at room temperature.

### **Statistical analysis**

Mechanical data was compared using Student's t-tests. MTT data were analyzed by single-factor ANOVA followed by a Tukey post-hoc test when appropriate. For comparisons between different distributions, Kolmogorov-Smirnov tests were used. All data are presented as mean ± standard deviation. An alpha level of p < 0.05 was considered significant.

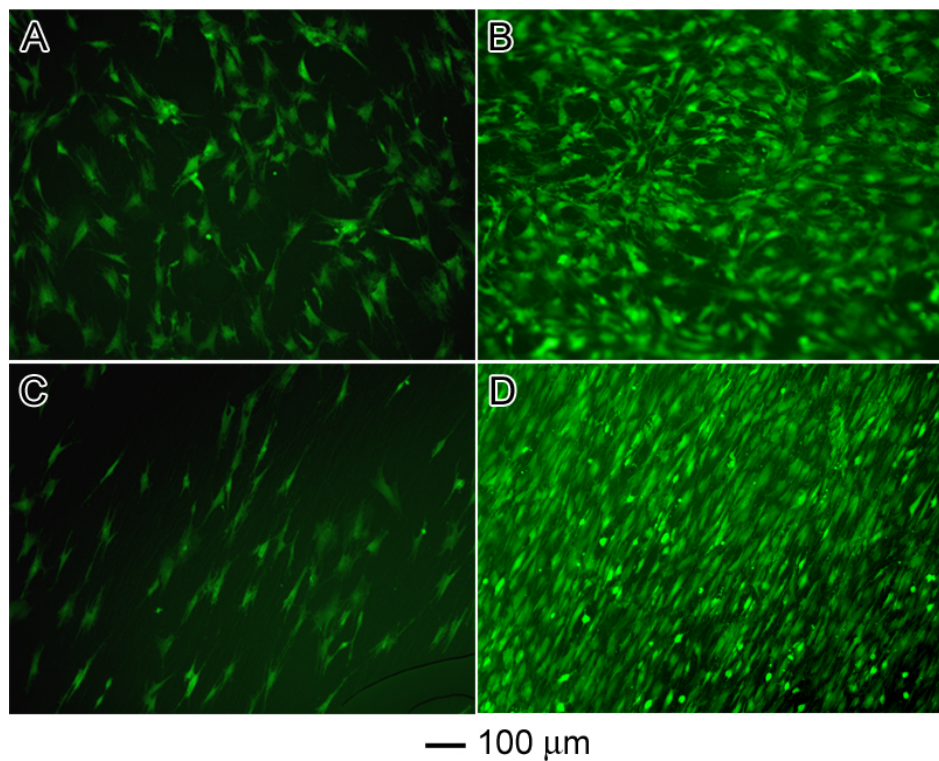


**Fig. S1.** Fluorescence micrographs showing cell morphology on fiber scaffolds: (A, B) random PLGA (50:50) fibers for 3 and 7 days, respectively; and (C, D) aligned PLGA (50:50) fibers for 3 and 7 days. Cells on the random scaffolds showed an irregularly shaped morphology with no preferred orientation. Cells on the aligned scaffolds showed an elongated morphology with a preferred orientation along the direction of fiber alignment.

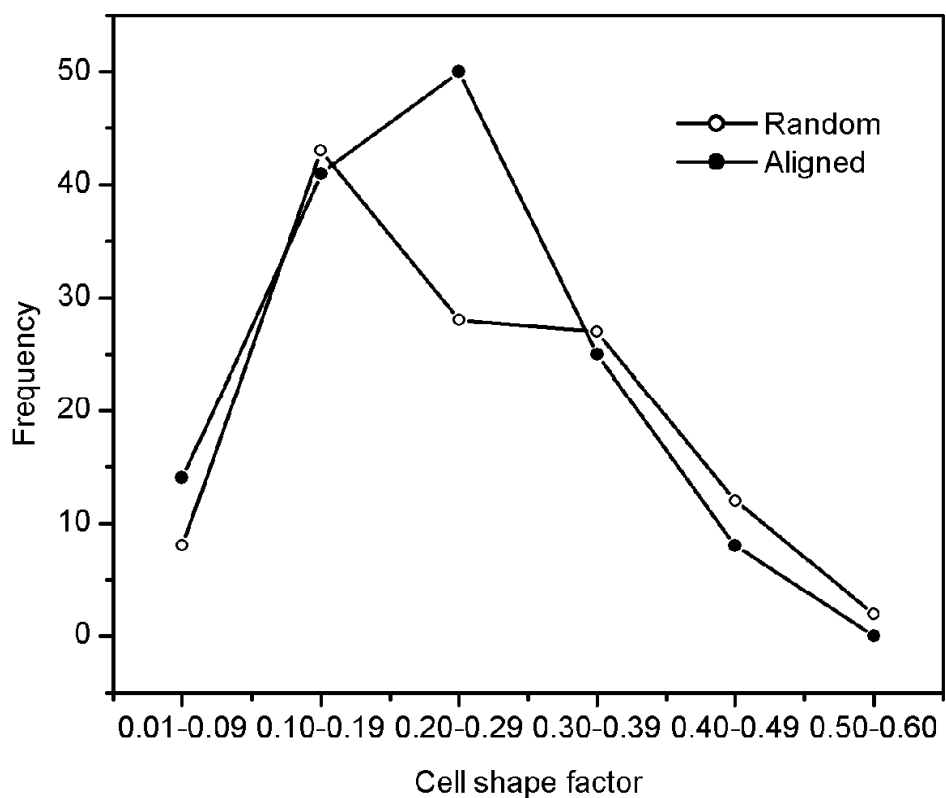


**Fig. S2.** Quantitative analysis of cell shape factor for cells cultured on random fiber scaffolds after incubation for 3 days.

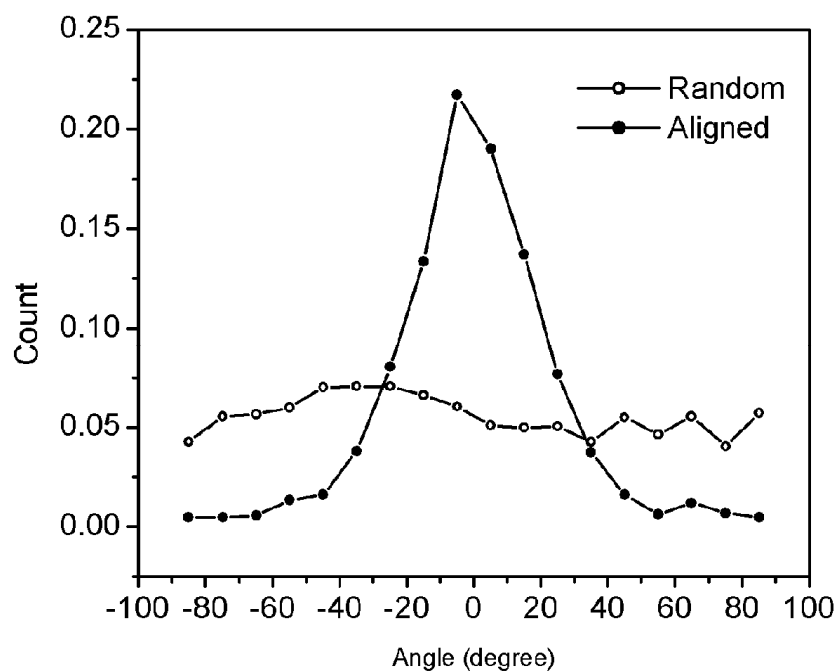


**Fig. S3.** Quantitative analysis of fibroblast response to PLGA (50:50) fiber scaffolds, respectively, after incubation for 3 days. The cell orientation distributions were significantly tighter (i.e., more aligned) on the aligned scaffolds.

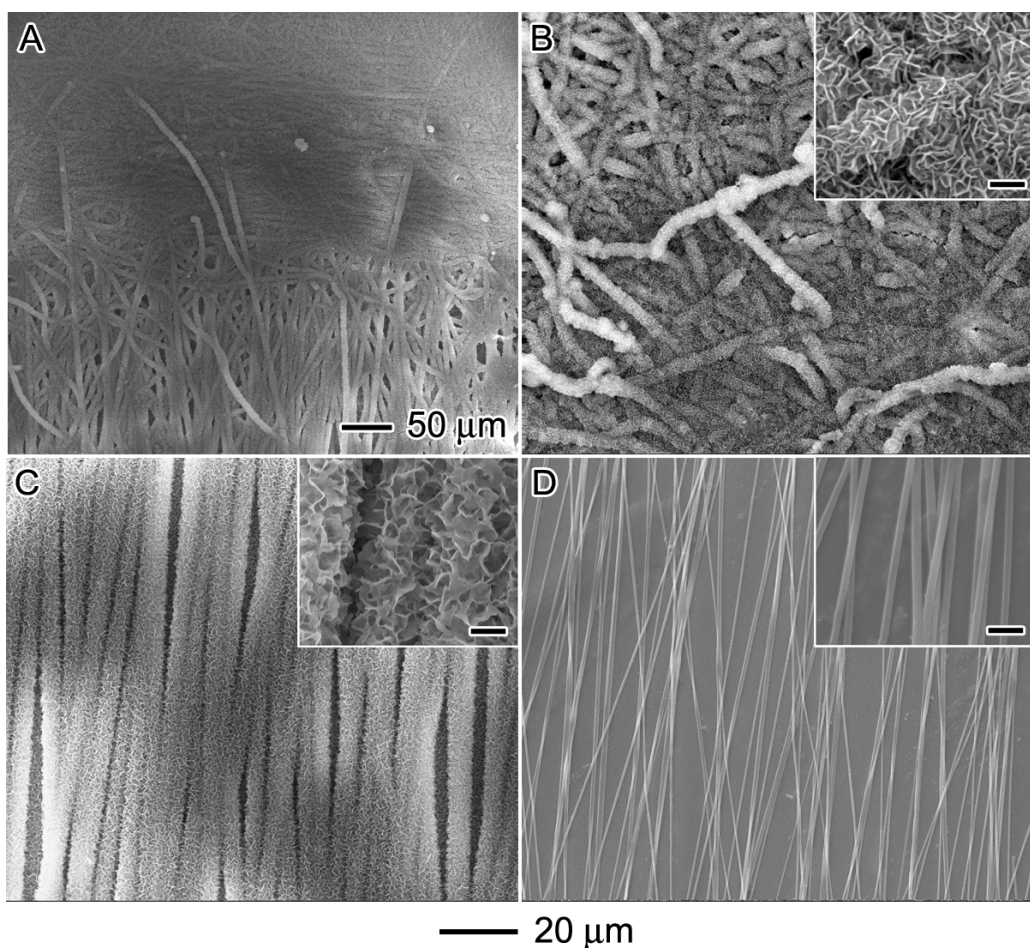


**Fig. S4.** SEM images of pre-mineralized “aligned-to-random” fiber scaffolds. A gradation in mineral can be seen at the interface between the random and aligned nanofibers (A). Higher magnification images show decreasing mineral content from the random side (B) to the aligned side (D) of the scaffold. The images were taken from different regions of the scaffold, corresponding to: (B) 0, (C) 5, and (D) 11 mm. The scale bars in the insets are 2  $\mu$ m.

## References:

- 1 J. Xie, M. R. MacEwan, X. Li, S. E. Sakiyama-Elbert, Y. Xia, *ACS Nano.*, 2009, **3**, 1151.
- 2 J. Xie, S. M. Willerth, X. Li, M. R. MacEwan, A. Rader, S. E. Sakiyama-Elbert, Y. Xia, *Biomaterials*, 2009, **30**, 354.
- 3 J. Xie, M. R. MacEwan, S. M. Willerth, X. Li, D. W. Moran, S. E. Sakiyama-Elbert, Y. Xia,

*Adv. Funct. Mater.*, 2009, **19**, 2312.

4 R. D. Robinson, L. J. Benjamin, J. M. Cosgriff, C. Cox, O. P. Lapets, P. T. Rowley, E. Yatco, L. L. Wheeless, *Cytometry*, 1994, **17**, 167.

5 W. J. Karlon, P. P. Hsu, S. Li, S. Chien, A. D. McCulloch, J. H. Omens, *Ann. Biomed. Eng.*, 1999, **27**, 712.